# Kinematic controllability and motion planning for the snakeboard

Francesco Bullo and Andrew D. Lewis

*Abstract*— **The snakeboard is shown to possess two decoupling vector fields, and to be kinematically controllable. Accordingly, the problem of steering the snakeboard from a given configuration at rest to a desired configuration at rest is posed as a constrained static nonlinear inversion problem. An explicit algorithmic solution to the problem is provided, and its limitations are discussed. An *ad hoc* solution to the nonlinear inversion problem is also exhibited.**

## I. Introduction

The snakeboard was first studied by Lewis et al., [1] and has since motivated a growing body of literature in robotics, control, and Lagrangian dynamics. The snakeboard is a challenging testbed for techniques aimed at modeling, controllability, gait analysis, and motion planning for mechanical control systems. It is a key example in the study of dexterous mechanical devices that exploit nonholonomic constraints to locomote.

In the initial work [1], various "gaits" were observed for the snakeboard which suggested that the system should be locally controllable. These gaits used periodic controls, and gave trajectories which, while interesting, are too complicated to use as tools for motion planning. The snakeboard was further studied by Ostrowski [2] using general techniques presented by Bloch et al., [3] for understanding the dynamics of mechanical systems with symmetry and constraints; see also [4]. Ostrowski [2] gave the first proof for the local controllability of the snakeboard (see also [5]). In [6] and [7] Ostrowski et al., investigate approximate planning algorithms and numerically generated optimal trajectories for the snakeboard. Until now, the goal of analytically determining steering controls for the snakeboard has not been achieved.

This goal is accomplished in this paper via the notion of kinematic controllability introduced by Bullo and Lynch [8]. This notion relies on the finding of a large enough collection of so-called "decoupling vector fields," i.e., vector fields whose integral curves can be followed with an arbitrary parameterisation. Motion planning can then be achieved by concatenating these integral curves starting and ending each integral curve at rest. The motion primitives we propose here do not generate nonholonomic momentum. This is in contrast to, for example, the work in [6], [7].

The contributions of this paper are organized as follows. In Section III, we show that the snakeboard is kinematically controllable. Note that this requires the slight extension of the original presentation of [8] to general affine connections (see also [9]), and this follows from the calculations in [10], [11] provided one is aware of the idea of kinematic controllability. In Section IV, we cast the motion planning problem for the snakeboard as a nonlinear inversion problem and we provide a constructive algorithmic solution. Furthermore, we discuss the advantages and limitations of the algorithm and exhibit a second *ad hoc* numerical solution. Note that our reduction of motion planning to a static, low-dimensional problem presents a significant computational improvement over methodologies which directly discretise the dynamic model, and perform optimisation on this model.

Coordinated Science Laboratory, University of Illinois at Urbana-Champaign, Urbana, IL 61801, U.S.A., email: bullo@uiuc.edu
Department of Mathematics & Statistics, Queen's University, Kingston, ON K7L 3N6, Canada, email: andrew@mast.queensu.ca

## II. The snakeboard model

The basis for our mathematical model for the snakeboard is illustrated in Figure 1. Its configuration space is coor-

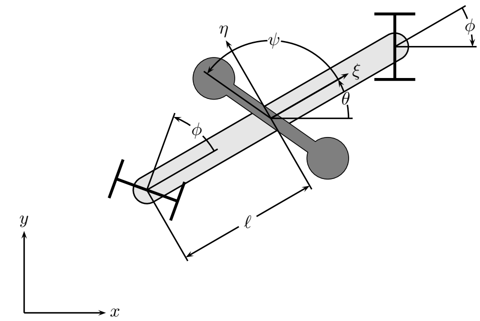


Fig. 1.

dinatized by $(x, y, \theta, \psi, \phi) \in Q = SE(2) \times \mathbb{S}^1 \times \mathbb{S}^1$. The inertia matrix for the snakeboard is given by

$$M = \begin{bmatrix} m & 0 & 0 & 0 & 0 \\ 0 & m & 0 & 0 & 0 \\ 0 & 0 & J + J_r + J_w & J_r & 0 \\ 0 & 0 & J_r & J_r & 0 \\ 0 & 0 & 0 & 0 & J_w \end{bmatrix},$$

where $m$ is the mass of the assembly, $J$ is the inertia of the snakeboard about its center of mass, $J_r$ is the rotor inertia, and $\frac{1}{2}J_w$ is the inertia of the wheels. This is a simplified model, but it captures the essential features of the system.

The snakeboard also has nonholonomic constraints which specify the admissible velocities at each configuration. One may readily show that the admissible velocities are spanned by the three vector fields

$$X_1 = \ell \cos(\phi) V_x - \sin(\phi) \frac{\partial}{\partial \theta},$$
$$X_2 = a(\phi) V_x - b(\phi) \frac{\partial}{\partial \theta} + \frac{\partial}{\partial \psi}, \quad X_3 = \frac{\partial}{\partial \phi},$$

where $V_x = \cos\theta \frac{\partial}{\partial x} + \sin\theta \frac{\partial}{\partial y}$ and

$$a(\phi) = \frac{J_r \ell \cos(\phi) \sin(\phi)}{c_1(\phi)}, \quad b(\phi) = \frac{J_r \sin^2(\phi)}{c_1(\phi)}, \qquad (1)$$
$$c_1(\phi) = m\ell^2 \cos^2(\phi) + (J + J_r + J_w) \sin^2(\phi).$$

We remark that the vector fields $X_1$, $X_2$, and $X_3$ are orthogonal with respect to the inertia matrix $M$. This orthogonality property is useful in writing the equations of motion for the snakeboard using the techniques in [11]. The inertia matrix and the constraints together define an affine connection $\nabla$ on $Q$ as related for the snakeboard by Lewis [12]. The unforced trajectories for the snakeboard are the geodesics of $\nabla$. The vector fields $\{X_1, X_2, X_3\}$ are orthogonal with respect to the inner product defined by the inertia matrix $M$. This allows us to use the simple formulae of Bullo and Žefran [11] to easily express the covariant derivatives of vector fields which lie in the constraint distribution. Of particular interest to us are the formulae

$$\nabla_{X_2} X_2 = 0, \quad \nabla_{X_3} X_3 = 0. \tag{2}$$

These are easily seen using the computations done for the snakeboard in [11], and we refer the reader there for details. We also remark that these computational details are available in the expanded preprint version of this paper [13].

The final element of the snakeboard model is the set of input forces. These are the forces arising from torques applied to the wheels and rotor. To express how these forces enter the equations of motion in the affine connection setting, we again refer the reader to [11]. Here we simply provide the result that the input forces are specified by the two vector fields

$$Y_\psi = \frac{c_1(\phi)}{J_r c_2(\phi)} X_2, \quad Y_\phi = \frac{1}{J_w} X_3, \tag{3}$$

where

$$c_2(\phi) = m\ell^2 \cos^2(\phi) + (J + J_w)\sin^2(\phi).$$

With this data, the snakeboard equations have the form

$$\nabla_{\dot q} \dot q = u_\psi Y_\psi(q) + u_\phi Y_\phi(q). \tag{4}$$

## III. Kinematic controllability of the snakeboard

The notion of kinematic controllability was introduced by Bullo and Lynch [8] motivated by the work in [14]. We consider general controlled mechanical systems that evolve according to equation (4) on an arbitrary configuration space $Q$ with a specified affine connection $\nabla$ and $m$ input vector fields $\{Y_1, \dots, Y_m\}$. For such a system, a vector field $X$ on $Q$ is a *decoupling vector field* if its integral curves may be followed, with an arbitrary reparameterization, by controlled trajectories for the mechanical system. Although Bullo and Lynch work only in the context of systems whose affine connection is Levi-Civita, their results are easily seen to apply to general affine connections, and so may be applied to the snakeboard equations (4). The main result of [8] (see also [9]) is the following.

**Proposition III.1** *A necessary and sufficient condition for a vector field $X$ to be a decoupling vector field is that both $X$ and $\nabla_X X$ should lie in the distribution spanned by the input vector fields $\{Y_1, \dots, Y_m\}$.*

Next, Bullo and Lynch [8] define a system to be *kinematically controllable* if it possesses decoupling vector fields $\{X_1, \dots, X_k\}$ whose involutive closure has maximal rank. The value of a system that is kinematically controllable is that one can do motion planning using concatenations of integral curves of the decoupling vector fields. The resulting concatenated curve, when reparameterized so that each segment begins and ends with zero velocity, will then be a trajectory for the mechanical system. Thus, one can essentially do the planning for a driftless system.

For the snakeboard, we have the following result.

**Lemma III.2** *The vector fields $X_2$ and $X_3$ are decoupling, and the involutive closure of the vector fields $\{X_2, X_3\}$ has maximal rank. In particular, the snakeboard is kinematically controllable.*

*Proof:* Note by (3) that $X_2$ is a multiple of $Y_\psi$ and that $X_3$ is a multiple of $Y_\phi$. Thus $X_2$ and $X_3$ take their values in the distribution spanned by the input vector fields. Also, by (2), the vector fields $\nabla_{X_2} X_2$ and $\nabla_{X_3} X_3$ trivially take their values in the input distribution. This shows that $X_2$ and $X_3$ are decoupling vector fields. A messy calculation shows that at all points in $Q$ where $\phi \notin \{\pm\frac{\pi}{4}, \pm\frac{3\pi}{4}\}$, the vector fields

$$\{c_1 X_2, X_3, [c_1 X_2, X_3], [X_3, [c_1 X_2, X_3]], [X_3, [c_1 X_2, [X_3, [c_1 X_2, X_3]]]]\}$$

span a distribution of maximal rank. At the degenerate values for $\phi$, the vector fields

$$\{c_1 X_2, X_3, [c_1 X_2, X_3], [X_3, [c_1 X_2, X_3]], [c_1 X_2, [X_3, [c_1 X_2, X_3]]]\}$$

span the tangent space. Since $c_1$ is an everywhere positive function, this shows that the involutive closure of $\{X_2, X_3\}$ has maximal rank as claimed. ■

## IV. Motion planning for the snakeboard

In this section we cast the motion planning problem for the snakeboard as a nonlinear inversion problem and we provide a constructive algorithmic solution. However, the algorithmic solution we provide will typically involve an unnecessarily large number of moves for the snakeboard. While we do not propose a systematic methodology to obtain satisfactory solutions to the motion planning problem, we do exhibit an *ad hoc* solution that demonstrates the potential value of solving the nonlinear inversion problem. The *ad hoc* solution of the problem that we determine is in closed form, although we do not discuss the details here. We also remark that, in contrast to the analysis of Ostrowski [6], the kinematic motions we use in our planning algorithm do not build nonholonomic momentum.

We first note that it is easy to alter $(\psi, \phi)$ to any desired position without altering $(x, y, \theta)$. Indeed, $\phi$ can be changed directly, and so too can $\psi$, provided one first sets $\phi = 0$. In this way we reduce our interest to achieving the desired values for $(x, y, \theta) \in SE(2)$. We do this by designing controls that steer from $(0, 0, 0)$ to points of the form

$(x_d, 0, 0)$, $(0, y_d, 0)$, and $(0, 0, \theta_d)$. The latter motion is obtained along with motion incurred in $x$ and $y$, but this can be corrected using the already obtained $x/y$-translations. By concatenating such motions, starting and ending at rest for each segment, we can achieve any desired configuration of the snakeboard.

### *A. The basic primitive*

Movement along the $X_3$ decoupling vector field is trivial; it merely specifies a rotation of the wheel angle $\phi$ without altering any of the other configurations. However, movement along the $X_2$ decoupling vector field is not so simple, and it is this motion which lies at the heart of our trajectory generation algorithm. Note that the components of $X_2$ depend on $\phi$. Therefore, to specify a motion along $X_2$, one should first specify a wheel angle $\phi = \phi_0$. The only other parameter in a movement along $X_3$ will then be the (signed) total time of the motion. Note that since the coefficient of $\frac{\partial}{\partial \psi}$ is 1 in $X_2$, the total time equals the change in the rotor angle $\Delta\psi$. What we shall determine is the relationship between $(\phi_0, \Delta\psi)$ and the motion in $(x, y, \theta) \in SE(2)$. To state this relationship, we utilize the definitions of $a(\phi)$ and $b(\phi)$ as given in (1). The reader may also wish to recall that, as a matrix group, $SE(2)$ consists of those matrices of the form

$$\begin{bmatrix} \cos(\theta) & -\sin(\theta) & x \\ \sin(\theta) & \cos(\theta) & y \\ 0 & 0 & 1 \end{bmatrix}, \quad x, y, \theta \in \mathbb{R}. \tag{5}$$

Furthermore, the Lie algebra $\mathfrak{se}(2)$ of this group consists of those matrices of the form

$$\begin{bmatrix} 0 & -\omega & \xi \\ \omega & 0 & \eta \\ 0 & 0 & 0 \end{bmatrix}, \quad \xi, \eta, \omega \in \mathbb{R}. \tag{6}$$

In the interests of compactness, let us represent the matrix (5) by $(x, y, \theta)$ and the matrix (6) by $(\xi, \eta, \omega)$. The Lie group exponential coincides with the matrix exponential, and is given in this case by

$$\exp(\xi, \eta, \omega) = \Big(\frac{\sin(\omega)}{\omega}\xi - \frac{1-\cos(\omega)}{\omega}\eta, \frac{1-\cos(\omega)}{\omega}\xi + \frac{\sin(\omega)}{\omega}\eta, \omega\Big),$$

when $\omega \neq 0$. With this notation, we have the following result.

**Lemma IV.1** *Let $q_0 = (0, 0, 0, 0, \phi_0) \in Q$ and let $(x, y, \theta, \Delta\psi, \phi_0) \in Q$ be the point obtained by flowing along $X_2$ for time $\Delta\psi$. Then*

$$\begin{aligned}(x, y, \theta) &= \exp\big(a(\phi_0)\Delta\psi, 0, -b(\phi_0)\Delta\psi\big) \\ &= \big(\ell \cot\phi_0 \sin(b(\phi_0)\Delta\psi), \\ &\quad \ell\cot\phi_0\big(\cos(b(\phi_0)\Delta\psi) - 1\big), b(\phi_0)\Delta\psi\big).\end{aligned}$$

*Proof:* The result follows from explicitly solving the differential equation associated with $X_2$ with $\phi = \phi_0$, and for time $\Delta\psi$. ■

It is evident from the definition of $X_2$ that during a motion along $X_2$, one should have $\phi_0 \notin \{0, \pi\}$ since in such a configuration the rotor will simply move without changing $(x, y, \theta)$. The following lemma describes the possible values of the quantities $a(\phi)\Delta\psi$ and $b(\psi)\Delta\psi$ obtainable using wheel angles between $-\frac{\pi}{2}$ and $\frac{\pi}{2}$.

**Lemma IV.2** *Let $S$ and $T$ be given by*

$$\begin{aligned} S &= \big(]-\tfrac{\pi}{2}, 0[\times]0, \tfrac{\pi}{2}[\big) \times (\mathbb{R} \setminus \{0\}) \\ T &= \mathbb{R}^2 \setminus (\{(x, 0) |\ x \in \mathbb{R}\} \cup \{(0, y) |\ y \in \mathbb{R}\}). \end{aligned}$$

*The map $(\phi, \Delta\psi) \mapsto (a(\phi)\Delta\psi, -b(\phi)\Delta\psi)$ is a diffeomorphism from $S$ to $T$.*

*Proof:* The differentiability of the stated map is clear. We can also produce an explicit inverse for the map:

$$(\xi, \omega) \mapsto \Big(-\arctan\big(\tfrac{\omega\ell}{\xi}\big), -\frac{c_1\big(\arctan\big(\frac{\omega\ell}{\xi}\big)\big)(\xi^2 + \ell^2\omega^2)}{J_r \ell^2 \omega}\Big).$$

This map is itself differentiable on the specified domain. ■

Combined, Lemmas IV.1 and IV.2 suggest that we should try to do motion planning in the coordinates $(x, y, \theta)$ using as parameters the forward and angular velocities $(\xi, \omega) = (a(\phi_0)\Delta\psi, b(\phi_0)\Delta\psi)$ constrained to the set $T$. For a physical snakeboard, it is reasonable to suppose that there will be restrictions on $\psi$ and $\phi$. For this reason, we make the assumption that $\psi \in [-\bar{\psi}, \bar{\psi}]$ and $\phi \in [-\bar{\phi}, \bar{\phi}]$ for some $\bar{\phi} \in ]0, \frac{\pi}{2}[$. This provides a restriction that $\|\Delta\psi\| \leq 2\bar{\psi}$. This then defines a set

$$\bar{S} = \big(]-\bar{\phi}, 0[\times]0, \bar{\phi}[\big) \times \big(]-2\bar{\psi}, 2\bar{\psi}[\big),$$

and the map of Lemma IV.2, when restricted to this set, will have an image as shown in Figure 2. The angle $\chi$ in

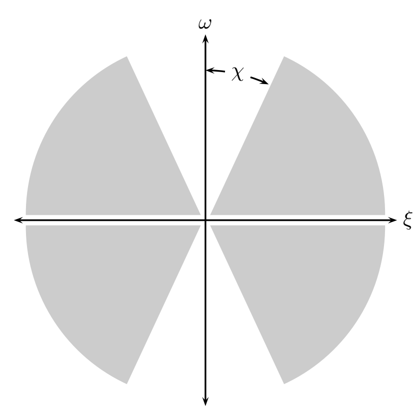


Fig. 2. The gray region describes the set of admissible values for the forward and angular velocities $(\xi, \omega)$ with constraints on the wheel and rotor angles

the figure is given by $\chi = -\arctan\big(\frac{\ell b(\bar{\phi})}{a(\bar{\phi})}\big)$. Let us denote by $\bar{T}$ the region of $\mathbb{R}^2$ shown in Figure 2.

### B. A nonlinear inversion problem for snakeboard motion planning, and an algorithmic solution

The idea of kinematic controllability is that one follows concatenations of integral curves of decoupling vector fields, ensuring that at the beginning and end of each segment, one is at rest. With the discussion of the preceding section as background, we can state the essence of the motion planning problem for the snakeboard as follows.

**Problem IV.3 (Snakeboard motion planning)** Suppose that $q_{\mathrm{i}} = (x_{\mathrm{i}}, y_{\mathrm{i}}, \theta_{\mathrm{i}}, \phi_{\mathrm{i}}, \phi_{\mathrm{i}})$ and $q_{\mathrm{f}} = (x_{\mathrm{f}}, y_{\mathrm{f}}, \theta_{\mathrm{f}}, \phi_{\mathrm{f}}, \phi_{\mathrm{f}})$ are given. Find a finite collection of points $(\xi_1, \omega_1), \ldots, (\xi_k, \omega_k) \in \bar{T}$ so that

$$(x_{\mathrm{i}}, y_{\mathrm{i}}, \theta_{\mathrm{i}}) \circ \exp(\xi_1, 0, \omega_1) \circ \cdots \circ \exp(\xi_k, 0, \omega_k) = (x_{\mathrm{f}}, y_{\mathrm{f}}, \theta_{\mathrm{f}})$$

(Here all terms are thought of as elements of $SE(2)$.) □

Of course, in obtaining a solution to the problem, one will want to minimize $k$. In the absence of control constraints, it is possible to show that one can steer from an initial configuration to any final configuration with $k$ at most 3. However, it appears quite difficult to analytically obtain such small bounds in the presence of constraints on the rotor and wheel angles.

Let us now turn to exhibiting a constructive algorithmic local solution to Problem IV.3. That is, for $(x_{\mathrm{f}}, y_{\mathrm{f}}, \theta_{\mathrm{f}})$ sufficiently close to $(0, 0, 0)$, we shall show how to steer from $(0, 0, 0)$ to the final point using a finite sequence of basic primitives. We do this essentially by demonstrating translations in the body $\xi$ and $\eta$-directions (see Figure 1), and then a rotation in $\theta$. The latter incurs motion in $x$ and $y$ which can be corrected by the already determined $\xi/\eta$-body translations. This gives rise to a complete closed-form local planner. It would be possible to design a global planner by computing appropriate sequences of desired local displacements and composing multiple invocations of the local planner.

*B.1. $\xi$-translation.* For a fixed $\phi_0 \neq 0$, we construct a sequence of three basic primitives as follows:

$$\begin{aligned}&\exp\big(a(\phi_0)\Delta\psi, 0, -b(\phi_0)\Delta\psi\big) \circ \\ &\quad \exp\big(2a(-\phi_0)\Delta\psi, 0, 2b(-\phi_0)\Delta\psi\big) \circ \\ &\quad\quad \exp\big(a(\phi_0)\Delta\psi, 0, -b(\phi_0)\Delta\psi\big) = (\Delta\xi, 0, 0).\end{aligned}$$

where

$$\Delta\xi = 4\ell \cot\phi_0 \sin\Big(\frac{J_r \Delta\psi \sin^2\phi_0}{c_1(\phi_0)}\Big).$$

For $\Delta\xi$ sufficiently small, we can compute the unique $\Delta\psi$ that will translate the snakeboard in body $\xi$-direction by an amount $\Delta\xi$. □

*B.2. $\eta$-translation.* For fixed $\phi_0 \neq 0$, we construct a sequence of four basic primitives as follows:

$$\begin{aligned}&\exp\big(a(\phi_0)\Delta\psi, 0, -b(\phi_0)\Delta\psi\big) \circ \\ &\quad \exp\big(-a(-\phi_0)\Delta\psi, 0, b(-\phi_0)\Delta\psi\big) \circ \\ &\quad \exp\big(-a(\phi_0)\Delta\psi, 0, b(\phi_0)\Delta\psi\big) \circ \\ &\quad \exp\big(a(-\phi_0)\Delta\psi, 0, -b(-\phi_0)\Delta\psi\big) = (0, \Delta\eta, 0),\end{aligned}$$

where

$$\Delta\eta = 4\ell \cot\phi_0 \Big(\cos\Big(\frac{J_r \Delta\psi \sin^2\phi_0}{c_1(\phi_0)}\Big) - 1\Big).$$

For $\Delta\eta$ sufficiently small, we can compute the unique $\Delta\psi$ that will translate the snakeboard in the body $\eta$-direction by an amount $\Delta\eta$. □

*B.3. $\theta$-specification.* The motion in the $\theta$-direction is achieved while incurring motion in the $x$ and $y$ variables as well. The single primitive we use is

$$\exp\big(a(\phi_0)\Delta\psi, 0, -b(\phi_0)\Delta\psi\big) = (\Delta x, \Delta y, \Delta\theta),$$

where

$$\begin{aligned}\Delta\theta &= -\frac{J_r \Delta\psi \sin^2\phi_0}{c_1(\phi_0)} \\ \Delta x &= \ell \cot\phi_0 \sin\Big(\frac{J_r \Delta\psi \sin^2\phi_0}{c_1(\phi_0)}\Big) \\ \Delta y &= \ell \cot\phi_0 \Big(\cos\Big(\frac{J_r \Delta\psi \sin^2\phi_0}{c_1(\phi_0)}\Big) - 1\Big).\end{aligned}$$

For a fixed $\phi_0 \neq 0$, we can compute the unique $\Delta\psi$ that will rotate the snakeboard by an amount $\Delta\theta$. Although there is an error in $x$ and $y$ variables, it can be corrected by employing the direct translations in these directions. Note that it *is* possible to produce a pure rotation by setting the wheel angles to $\pm\frac{\pi}{2}$, and then following $X_3$. We do not allow this as we wish to guarantee that the wheel angles can be kept small. □

In Figure 3 we show a motion of the snakeboard from $(x, y, \theta) = (0, 0, 0)$ to $(x, y, \theta) = \big(\sqrt{2}, 2, \frac{\pi}{5}\big)$. The rotation by $\frac{\pi}{5}$ was broken into two smaller rotations to mollify the effects of the deviation in $x$ and $y$. We note that, including final corrections to the wheel and rotor angles, the above sort of motion will involve a concatenation of twenty basic kinematic motions.

*B.4. An* ad hoc *solution to the nonlinear inversion problem.* The above procedure demonstrates an algorithmic solution to Problem IV.3, albeit a rather inefficient one. One can also proceed by looking directly at the equations yielded by Problem IV.3. Without the constraints on the wheel and rotor angles, it is possible to construct a procedure that will steer the snakeboard between two $(x, y, \theta)$ configurations using a concatenation of at most three basic primitives. One can do this by looking at the equations generated by the problem, noting that for three primitives there will be six independent variables (three pairs $(\xi, \omega)$).

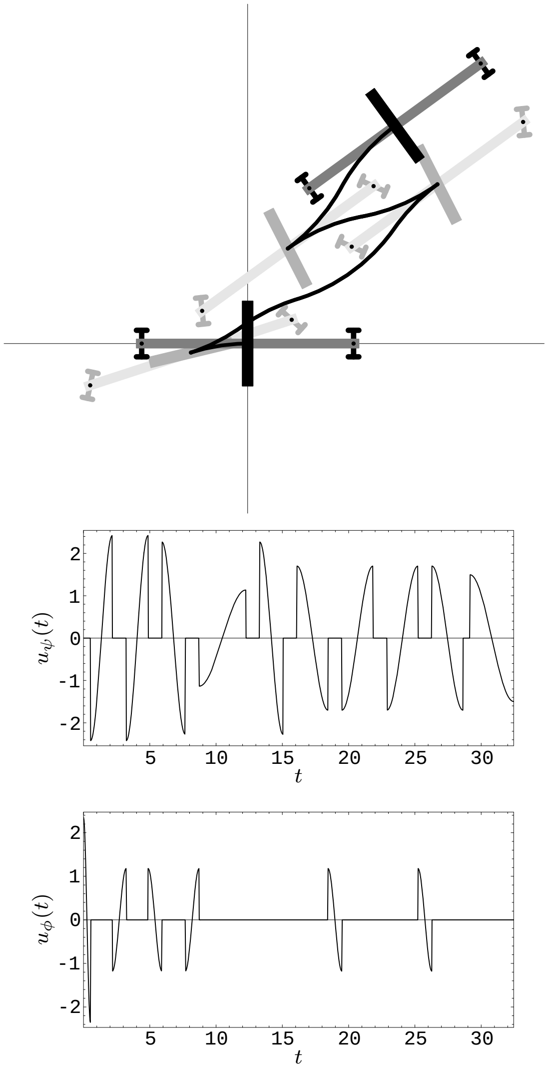


Fig. 3. Snakeboard motion from $(0,0,0)$ to $\left(\sqrt{2}, 2, \frac{\pi}{5}\right)$ using concatenations of basis primitives. The controls are shown in the bottom figure. The parameters used are $(m, \ell, J, J_r, J_w) = (1, 1, 1, 1, \frac{1}{4})$.

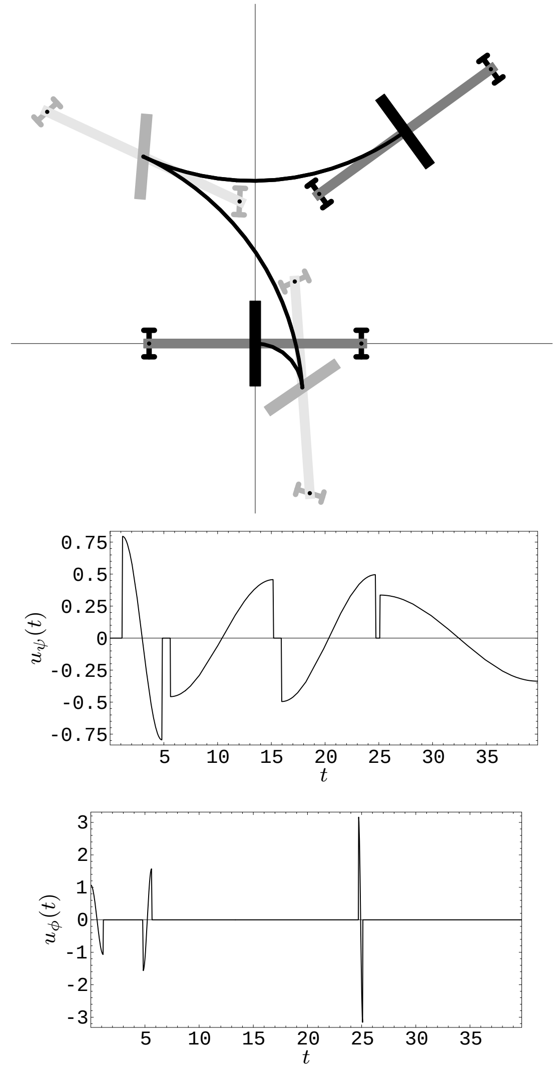


Fig. 4. Snakeboard motion from $(0,0,0)$ to $\left(\sqrt{2}, 2, \frac{\pi}{5}\right)$ using an *ad hoc* solution to Problem IV.3. The controls are shown in the bottom figure. The parameters used are $(m, \ell, J, J_r, J_w) = (1, 1, 1, 1, \frac{1}{4})$.

One can then impose relations on these variables to reduce the extent to which the problem is under-determined. In this way, various sorts of *ad hoc* procedures are fairly easily developed. However, it appears to be difficult to do this in a methodical way so that the wheel and rotor angle constraints are satisfied. In Figure 4 we show such a three primitive motion, steering to the same final point as was done in Figure 3.

**Remarks IV.4** 1. For the purposes of making more easily understood plots, we have ignored constraints of the rotor angle $\psi$. When constraints on this angle are enforced, the motions become comparatively smaller than those in Figures 3 and 4.
2. For an accurate comparison of the motion in Figure 4 with the motion of Figure 3, we should also count the motions involving positioning the wheels, and straightening out the rotor and wheels after the motion. In this case, there are eight segments of the motion in Figure 4, compared with twenty for the motion in Figure 3. □

## V. Discussion

The snakeboard is a somewhat simple example of a mechanical system, and yet it is certainly not trivial. Indeed, until now, the motion planning problem for the snakeboard has resisted any sort of non-numerical solution. In this paper we have shown that it is possible to reduce the motion planning problem for the snakeboard to a low-dimensional static nonlinear inversion problem. Although this problem is not of particularly pleasing nature, we have shown that it admits a closed form solution by constructing an algorithmic local motion planning strategy.

We conclude by remarking on the advantages of the affine connection formalism in the modeling and control theory for mechanical systems. Indeed, it is in this setting that the notions of decoupling vector fields and kinematic controllability are naturally understood. It is also worth noting that the idea of decoupling vector fields arises in an interesting and nontrivial way in the quadratic form controllability conditions of Hirschorn and Lewis [15]. This is an interesting avenue for further research.

## References


[1] A. D. Lewis, J. P. Ostrowski, R. M. Murray, and J. W. Burdick, "Nonholonomic mechanics and locomotion: the Snakeboard example," in *Proceedings of the IEEE ICRA*, San Diego, May 1994, IEEE, pp. 2391–2400.

[2] J. P. Ostrowski, *The Mechanics and Control of Undulatory Robotic Locomotion*, Ph.D. thesis, California Institute of Technology, Pasadena, California, USA, Sept. 1995.

[3] A. M. Bloch, P. S. Krishnaprasad, J. E. Marsden, and R. M. Murray, "Nonholonomic mechanical systems with symmetry," *Arch. Rational Mech. Anal.*, vol. 136, no. 1, pp. 21–99, 1996.

[4] W. S. Koon and J. E. Marsden, "Optimal control for holonomic and nonholonomic mechanical systems with symmetry and Lagrangian reduction," *SIAM J. Control Optim.*, vol. 35, no. 3, pp. 901–929, 1997.

[5] J. P. Ostrowski and J. W. Burdick, "Controllability tests for mechanical systems with constraints and symmetries," *J. Appl. Math. and Comp. Sci.*, vol. 7, no. 2, pp. 101–127, 1997.

[6] J. P. Ostrowski, "Steering for a class of dynamic nonholonomic systems," *IEEE Trans. Automat. Control*, vol. 45, no. 8, pp. 1492–1497, 2000.

[7] J. P. Ostrowski, J. P. Desai, and V. Kumar, "Optimal gait selection for nonholonomic locomotion systems," *Internat. J. Robotics Res.*, vol. 19, no. 5, pp. 225–237, 2000.

[8] F. Bullo and K. M. Lynch, "Kinematic controllability and decoupled trajectory planning for underactuated mechanical systems," *IEEE Trans. Robotics and Autom.*, vol. 17, no. 4, pp. 402–412, 2001.

[9] J. Cortés, S. Martínez, and F. Bullo, "On nonlinear controllability and series expansions for Lagrangian systems with dissipative forces," *IEEE Trans. Automat. Control*, vol. 47, no. 8, pp. 1396–1401, 2002.

[10] A. D. Lewis, "Simple mechanical control systems with constraints," *IEEE Trans. Automat. Control*, vol. 45, no. 8, pp. 1420–1436, 2000.

[11] F. Bullo and M. Žefran, "On mechanical systems with nonholonomic constraints and symmetries," *Systems Control Lett.*, vol. 45, no. 2, pp. 133–143, 2002.

[12] A. D. Lewis, "Affine connections and distributions with applications to nonholonomic mechanics," *Rep. Math. Phys.*, vol. 42, no. 1/2, pp. 135–164, 1998.

[13] F. Bullo and A. D. Lewis, "Kinematic controllability and motion planning for the snakeboard," Preprint, Dec. 2001, available online at `http://penelope.mast.queensu.ca/~andrew/`.

[14] K. M. Lynch, N. Shiroma, H. Arai, and K. Tanie, "Collision-free trajectory planning for a 3-DOF robot with a passive joint," *Internat. J. Robotics Res.*, vol. 19, no. 12, pp. 1171–1184, 2000.

[15] R. M. Hirschorn and A. D. Lewis, "Geometric first-order controllability conditions for affine connection control systems," in *Proceedings of the 39th IEEE CDC*, Orlando, FL, Dec. 2001, IEEE, pp. 4216–4221.